

Secular Dynamics of Three-Body Systems and the Origins of Retrograde Hot Jupiters

Senior Thesis in Physics & Astronomy

Ian Lizarraga

Advisors: Professor Fred Rasio & Doctor Smadar Naoz

May 16, 2011

Prepared in partial fulfillment of the requirements for the Honors Degree in Physics

Northwestern University

Abstract

We consider the secular-perturbation expansion of the classical Hamiltonian equations of motion for three mutually gravitating bodies, and we use the formalism to study the dynamical evolution of hierarchical three-body systems to octupole-level accuracy. Our study is partly motivated by recent observations of exoplanetary systems, which may include two giant planets strongly perturbing each other gravitationally on secular timescales. These systems display a rich array of dynamics not present in the commonly adopted quadrupole-level models. In particular, long-period, large-amplitude oscillations in the eccentricity e_1 and inclination i_1 of the inner orbit have been observed. In some cases the inner orbit may even become *retrograde*, providing a possible explanation of the “retrograde Hot Jupiters” that have been observed recently in several systems. We study in some detail the mechanisms giving rise to such retrograde orbits and we propose a model that may apply to the entire phase space. We find that the probability to induce a flip in the inner binary is highly dependent on the maximum inner orbit eccentricity e_1 reached during the dynamical evolution of the system. We also find that the probability to reach high eccentricities increases with time and, as a result, the probability for a flip approaches unity (formally, over an infinite time) above a certain threshold in $e_{1,\max}$. Finally we show that the relationship between the quadrupole- and octupole-level secular timescales plays an important role in setting the probability to reach high eccentricities (over some finite time) and thus to flip the inner orbit.

1 Introduction

Understanding the trajectories of three mutually gravitating bodies is a famous problem in physics. Extremely easy to formulate yet nearly impossible to solve in all but the simplest cases, the problem even prompted King Oscar II of Sweden to establish a prize in 1887 for anyone who could provide a complete solution (Valtonen and Karttunen, 2006). Since the 1800's a complete series solution to the N -body problem (for $N \geq 3$) has been found (Wang, 1991), but the convergence of terms to the exact solution is so slow that the study of a reasonable truncation illuminates very little of the corresponding dynamics. Constraining the problem to astrophysically significant configurations and parameter ranges, as well as invoking the power of numerical integration, makes it feasible for researchers to understand the behavior of more interesting systems over relevant astronomical timescales.

We concentrate on *hierarchical* triple systems, which produce a wide variety of interesting phenomena. Triple star systems are believed to be very common (e.g., Eggleton *et al.*, 2007; Tokovinin, 1997). The hierarchical triple configuration, consisting of an inner binary in conjunction with a third body on a much wider orbit, is a dynamically stable astrophysical configuration, so we expect such systems to exist. In fact, more than 50% of bright stars have been found to exist in at least a double configuration (Eggleton *et al.*, 2007; Tokovinin, 1997). Given the selection effects against finding faint and distant companions we can be reasonably confident that the fraction of astrophysical N -body systems for $N \geq 2$ is actually much larger. Tokovinin (1997) showed that 40% of binary stars with period < 10 d in which the primary is a dwarf ($0.5 - 1.5M_{\odot}$) have at least one additional companion. He found that the fraction of triples and higher multiples among binaries with period (10 – 100 d) is $\sim 10\%$. Moreover, Pribulla and Rucinski (2006) have shown that among a sample of 151 contact binaries brighter than 10 mag., $42 \pm 5\%$ are at least triple.

Another compelling reason to study the dynamics of hierarchical triples is that many close stellar binaries with two compact objects were likely produced through the evolution of a triple. Unique behaviors present in a triple's *secular* evolution (i.e., evolution occurring on timescales that are very long compared to the orbital periods), specifically, the occurrence of Kozai cycling (which will be discussed below) has been proposed as an important element in the evolution of triple stars (e.g., Mazeh and Shaham, 1979; Kiseleva *et al.*, 1998; Fabrycky and Tremaine, 2007; Perets and Fabrycky, 2009). In addition, Kozai cycling has been suggested to play an important role in both the growth of black holes at the centers of dense star clusters and the formation of short-period binary black holes (Wen, 2003; Miller and Hamilton, 2002; Blaes *et al.*, 2002).

Secular perturbations in triple systems also play an important role in solar system dynamics. Kozai (1962) studied the gravitational perturbations on an inclined asteroid that arises from Jupiter in our solar system. In this hierarchical configuration the asteroid, a test particle, exhibits fluctuations in its inclination and eccentricity over secular timescales. Recently it was also shown that considering minor planets in binaries as the component of a triple configuration, where the third body is the sun, can be very useful in understanding present

day observations. For instance, the evolution of binary minor planets has been shown to be influenced by secular gravitational perturbations from the sun (Perets and Naoz, 2009).

The hierarchical triple configuration has also been shown to be very useful in studying the evolution of extrasolar planets (e.g., Innanen *et al.*, 1997; Wu and Murray, 2003; Fabrycky and Tremaine, 2007; Wu *et al.*, 2007; Takeda *et al.*, 2008; Naoz *et al.*, 2011). Recent discoveries made by the *Kepler* satellite emphasize the importance of the hierarchical triple configuration in the context of planetary systems. More than 1200 candidates for exoplanets have been identified (Borucki *et al.*, 2011); thus, it seems inevitable that statistical analysis will reveal a host of properties characteristic of these systems, which include many multi-planet configurations. Therefore, in anticipation of the upcoming datasets, it is highly desirable to develop a useful theoretical formalism that can account for the unusual orbital properties observed for many of these planets (see Naoz *et al.*, 2011, also see below for more details).

Recent observations using the Rossiter-McLaughlin effect (Gaudi and Winn, 2007) have shown that about 25% of hot Jupiters (extrasolar Jovian-mass planets with close-in orbits, hereafter HJs) are actually orbiting *counter* to the spin direction of the star (Triaud *et al.*, 2010). Let us briefly summarize the use of the RM effect to validate these claims. Doppler shifting of light implies that a star’s atmosphere is bluer coming toward us and redder going away from us— therefore, during transits, the spin of the star produces a small spectroscopic shift of the light received by a telescope as the transiting planet obscures either the red-shifted or blue-shifted side of the stellar disk. This spectroscopic signal allows us to determine whether the orbit is prograde or retrograde (see Fig. 1).

Despite many attempts (Fabrycky and Tremaine, 2007; Wu *et al.*, 2007; Chatterjee *et al.*, 2008; Lai *et al.*, 2010; Nagasawa *et al.*, 2008; Takeda *et al.*, 2008; Winn *et al.*, 2010), there is no model that can account for all the properties of the known HJ systems. One model suggests that HJs were formed far away from the star and slowly spiraled in, losing angular momentum and orbital energy to the protoplanetary disk (Lin and Papaloizou, 1986; Masset and Papaloizou, 2003). However, this “migration” process should produce planets with low orbital inclinations and eccentricities, similar to the configuration seen in our own solar system. However, many HJs are observed to be on orbits with high eccentricities, and furthermore are misaligned with the spin direction of the star. Naoz *et al.* (2011) showed that when tidal forces are taken into account, a system composed of a star and a Jovian planet (the inner binary) being perturbed by a distant outer planet can induce capture, bringing the Jupiter planet into very close proximity to the star, while also changing its inclination and sometimes flipping its orientation completely.

The inducement of flips in the inner orbit from purely dynamical effects (especially the prospect of correlating retrograde motion with highly eccentric orbits) is very promising and is the subject of this study. We consider neither general relativistic nor tidal effects on the resulting orbital motion. We expect relativistic precession of the inner orbit and the inclusion of tidal forces could change the dynamics in some cases. For example, the Kozai capture mechanism alluded to above predicts the decay of the semimajor axis of the inner orbit

principally due to tidal friction. Nevertheless, it is very useful to first study theoretically the point-mass Newtonian dynamics of these systems. This follows the usual approach in nonlinear dynamics of first understanding the non-dissipative dynamics of complex systems.

This thesis is organized as follows. In Sec. 2 we briefly summarize previous work on the Hamiltonian equations of motion for the three-body problem before motivating and deriving the Hamiltonian up to octupole order. In Sec. 3 we present and discuss our numerical results. Finally we conclude and discuss future directions for research in Sec. 4.

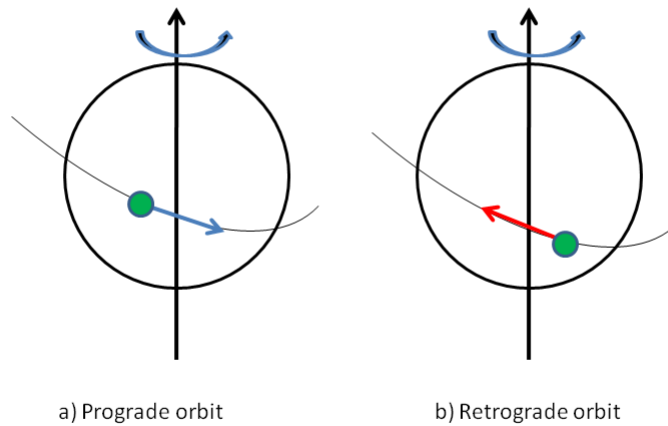


Fig. 1: Visual description of a) a prograde and b) a retrograde orbit. The central black arrows in both of the diagrams depict the direction $\mathbf{L}_{\text{tot}} \parallel \hat{z}$, the total angular momentum of the system, which is assumed to be aligned with the spin momentum of the star. The blueshifted side is obscured first (so we observe redshift first) in case a), and *vice versa* in case b).

2 The Hamiltonian and Equations of Motion

The Hamiltonian of a mutually gravitating three-body system can be written in a way that recalls the multipole expansion in electrostatics. Kozai's seminal work (Kozai, 1962) implemented classical perturbation theory and provided a satisfactory description of an asteroid moving under the attraction of the Sun and Jupiter. Among the surprising dynamics arising from his *quadrupole*-level analyses were the occurrence of librations and oscillations of eccentricities and inclinations among the inner and outer orbits, effectively limiting their values between well-defined bounds for any given initial condition. In fact the periodic exchange between the inclination and eccentricity of the orbit can be encapsulated in the now canonical *Kozai constant* H_{Koz} through the elegant relation $H_{Koz} = \sqrt{a(1-e^2)} \cos i$ (see for eg. Verrier and Evans (2008) or Valtonen and Karttunen (2006) for a derivation). However, it

was shown (Naoz *et al.*, 2011) that perturbation theory up to the quadrupole level is not sufficient to account for the possibility of an orbit to flip from prograde to retrograde. It turns out that by carefully extending the perturbatory analysis up to octupole order, we arrive at equations of motion that do allow for this possibility. Therefore we proceed by illustrating the theory of the octupole-level equations.

Following Naoz *et al.* (2011), let m_1 and m_2 be the masses of the close binary and let m_3 be the mass of the third body. Define \mathbf{r}_1 to be the vector from m_1 to m_2 and let \mathbf{r}_2 be the vector from the center of mass of the inner binary to m_3 . We transform to the more geometric *orbital elements* $(\tau_j, a_j, e_j, i_j, \omega_j, \Omega_j)$, where $j = 1(i), 2(e)$ for the inner or outer orbit, respectively. Here, τ_j is the mean anomaly, a_j is the semi-major axis, e_j is the eccentricity, i_j is the inclination with respect to the total angular momentum G_{tot} of the system, ω_j is the argument of pericenter, and Ω_j is the longitude of the ascending node of the inner or outer orbit, respectively. Finally, we denote the gravitational constant by k^2 . The reader may refer to Fig. 2 for more details.

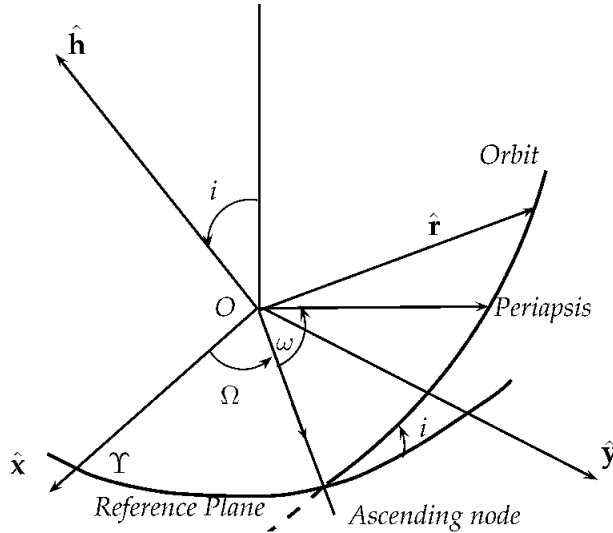


Fig. 2: With permission from J. Teyssandier. A visual description of the orbital elements (Ω, ω, i) as well as the reference plane and orbits. For the hierarchical system we consider two planes distinct from the reference plane. Later we set our reference plane to be the *invariable* plane, defined to be the plane perpendicular to the total angular momentum vector of the system.

With these definitions it is straightforward to write the Hamiltonian of the system in terms of these variables, expanding the Newtonian gravitational potential $V = k^2/|\mathbf{r}_i - \mathbf{r}_j|$ in a power series of $\alpha = a_1/a_2$ (called for obvious reasons a *multipole expansion* (Harrington, 1969)):

$$\mathcal{H} = \frac{k^2 m_1 m_2}{2a_1} + \frac{k^2 m_3 (m_1 + m_2)}{2a_2} + \frac{k^2}{a_2} \sum_{j=2}^{\infty} \alpha_j M_j \left(\frac{r_1}{a_1}\right)^j \left(\frac{r_2}{a_2}\right)^{j+1} P_j(\cos \Phi), \quad (1)$$

where P_j are the Legendre polynomials, Φ is the angle between \mathbf{r}_1 and \mathbf{r}_2 , and

$$M_j = m_1 m_2 m_3 \frac{m_1^{j-1} - (-m_2)^{j-1}}{(m_1 + m_2)^j}. \quad (2)$$

Recalling the analogy with electrostatics, the $j = 2$ term in the sum is defined as the *quadrupole* term and the $j = 3$ term is defined as the *octupole* term. We can find an even more convenient set of canonically conjugate variables to describe our hierarchical triple, namely *Delaunay's elements*. We let

$$\begin{aligned} l_{1,2} &= M_{1,2}, \\ h_{1,2} &= \Omega_{1,2}, \text{ and} \\ g_{1,2} &= \omega_{1,2}, \end{aligned} \quad (3)$$

where $M = n(t - \tau)$ is the mean anomaly. Via a suitable generating function (Valtonen and Karttunen, 2006) we obtain their conjugate momenta:

$$\begin{aligned} L_1 &= \frac{m_1 m_2}{m_1 + m_2} \sqrt{k^2 (m_1 + m_2) a_1}, \\ L_2 &= \frac{m_3 (m_1 + m_2)}{(m_1 + m_2 + m_3)} \sqrt{k^2 (m_1 + m_2 + m_3) a_2}, \\ G_1 &= L_1 \sqrt{1 - e_1^2}, \\ G_2 &= L_2 \sqrt{1 - e_2^2}, \\ H_1 &= G_1 \cos i_1, \text{ and} \\ H_2 &= G_2 \cos i_2. \end{aligned} \quad (4)$$

Adopting the coordinate system where the total initial angular momentum lies along the z -axis (the invariable plane), we note that G_1 and G_2 are the absolute values of the angular momentum vectors \mathbf{G}_1 and \mathbf{G}_2 , and $H_{1,2}$ is the z -component of angular momentum of the inner (resp. outer) orbit. Taking the dot product of appropriate vectors and using trivial trigonometry immediately give us two useful identities relating these magnitudes:

$$H_{1,2} = \frac{G_{\text{tot}}^2 + G_{1,2}^2 - G_{2,1}^2}{2G_{\text{tot}}}. \quad (5)$$

Next we relate the generalized coordinates and momenta (eqs. (3) and (4)) by the usual canonical equations of motion (which the careful reader will note are actually *minus* the standard equations simply due to a convention made by Harrington (1969), giving us a

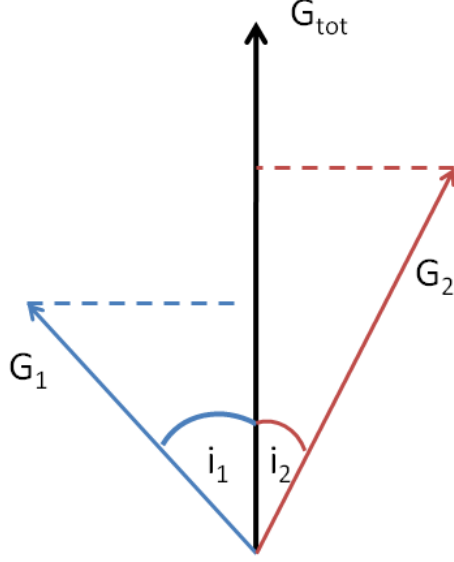


Fig. 3: A visual description of the equations (5). Here G_{tot} is the total angular momentum, which we choose to lie in the \hat{z} direction. G_1 and G_2 are the angular momenta of the inner and outer orbits, respectively (which we place arbitrarily in the figure). Finally, $i = i_1 + i_2$ is the angle between G_1 and G_2 (not shown here explicitly).

nonnegative energy):

$$\begin{aligned}
\frac{dL_i}{dt} &= \frac{\partial \mathcal{H}}{\partial l_i}, \\
\frac{dG_i}{dt} &= \frac{\partial \mathcal{H}}{\partial g_i}, \\
\frac{dH_i}{dt} &= \frac{\partial \mathcal{H}}{\partial h_i}, \\
\frac{dl_i}{dt} &= -\frac{\partial \mathcal{H}}{\partial L_i}, \\
\frac{dg_i}{dt} &= -\frac{\partial \mathcal{H}}{\partial G_i}, \text{ and} \\
\frac{dh_i}{dt} &= -\frac{\partial \mathcal{H}}{\partial H_i}.
\end{aligned} \tag{6}$$

At this point we may rewrite the Hamiltonian *through octupole accuracy* as (Ford *et al.*, 2000):

$$\begin{aligned}
\mathcal{H} &= \frac{\beta_0}{2L_1^2} + \frac{\beta_1}{2L_2^2} + 8\beta_2 \left(\frac{L_1^4}{L_2^6} \right) \left(\frac{r_1^2}{a_1^2} \right) \left(\frac{a_2^3}{r_2^3} \right) (3 \cos^2 \Phi - 1) + \\
&2\beta_3 \left(\frac{L_1^6}{L_2^8} \right) \left(\frac{r_1^3}{a_1^3} \right) \left(\frac{a_2^4}{r_2^4} \right) (5 \cos^3 \Phi - 3 \cos \Phi),
\end{aligned} \tag{7}$$

where the parameters β_i are given by

$$\begin{aligned}
\beta_0 &= k^4 \frac{m_1^3 m_2^3}{m_1 + m_2}, \\
\beta_1 &= k^4 \frac{(m_1 + m_2)^3 m_3^3}{(m_1 + m_2 + m_3)}, \\
\beta_2 &= \frac{k^4 (m_1 + m_2)^7}{16 (m_1 + m_2 + m_3)^3}, \text{ and} \\
\beta_3 &= \frac{k^4 (m_1 + m_2)^9}{4 (m_1 + m_2 + m_3)^4} \frac{m_2^9 (m_1 - m_2)}{m_1^5 m_2^5}.
\end{aligned} \tag{8}$$

We are interested only in the secular, long-term behavior of the system as mentioned in the introduction. Therefore we may average the Hamiltonian \mathcal{H} over the mean anomalies l_1 and l_2 in a well-defined canonical way (the *von Zeipel transformation*) by setting our new, averaged Hamiltonian equal to the old one and identifying terms in the Taylor series (Goldstein *et al.*, 2001). We omit the details and present here only the results derived by Ford *et al.* (2000) after the double-averaging process. We define $i = i_1 + i_2$ to be the total inclination of the orbits, and write out the doubly-averaged Hamiltonian H' in the limiting case of $G_2 \gg G_1$ and $i_2 \rightarrow 0$, since this is the case we shall be studying:

$$\begin{aligned}
H' &= C_2[(2 + 3e_1^2)(3 \cos^2 i - 1) + 15e_1^2 \sin^2 i \cos 2g_1] \\
&\quad + C_3 e_1 e_2 [A \cos \varphi + 10 \cos i \sin^2 i (1 - e_1^2) \sin g_1 \sin g_2],
\end{aligned} \tag{9}$$

where

$$\cos \varphi = -\cos g_1 \cos g_2 - \cos i \sin g_1 \sin g_2, \tag{10}$$

$$C_2 = \frac{k^4 (m_1 + m_2)^7}{16} \frac{m_2^7}{M_0^3} \frac{L_1^4}{(m_1 m_2)^3 L_2^3 G_2^3}, \tag{11}$$

$$C_3 = -\frac{15}{4} \frac{m_1 - m_2}{(m_1 + m_2 + m_3)} \left(\frac{m_2 (m_1 + m_2)}{m_1 m_2} \right)^2 \frac{L_1^2}{G_2^2} C_2, \tag{12}$$

$$B = 2 + 5e_1^2 - 7e_1^2 \cos 2g_1, \text{ and} \tag{13}$$

$$A = 4 + 3e_1^2 - \frac{5}{2} B \sin^2 i. \tag{14}$$

We should note that this Hamiltonian [eq. (9)] is incomplete. The absence of $h_{1,2}$ from the equation does not necessarily imply that the z-components of the angular momenta $H_{1,2}$ are constant, as we may naïvely assume from the Hamiltonian equations of motion. However, one can use this Hamiltonian in order to derive the equations of motion, as long as one remembers that $H_{1,2}$ are not constant. The equations of motion for these variables (and therefore the inclinations) can be derived using the total momentum conservation law [eq. (5)].

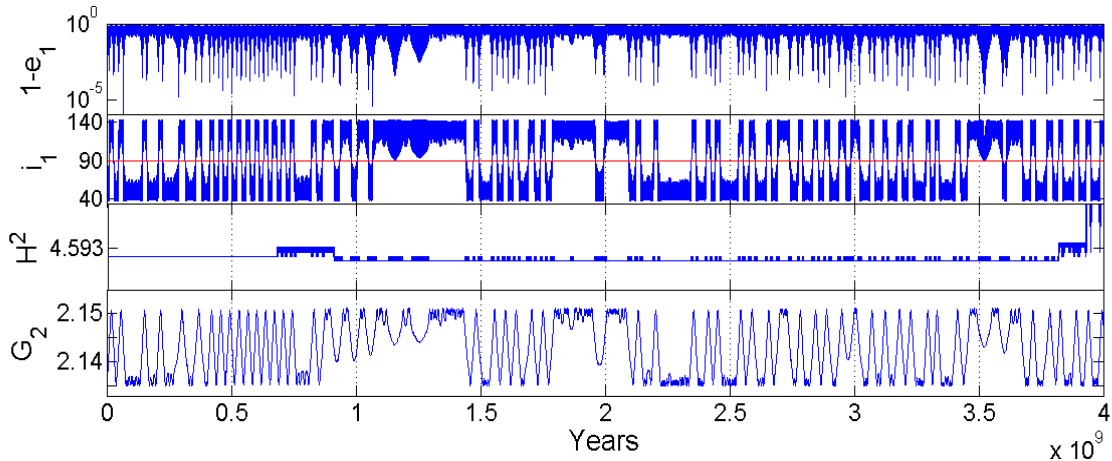
3 Numerical Simulations

Numerical simulations were carried out using the *Octupole-Level Secular Perturbation Equations* (OSPE) package (Ford *et al.*, 2000). OSPE integrates the equations of motion derivable from eq. (9) using the Bulirsch-Stoer algorithm. We focused on a two-planet model of the type motivated in Sec. 1. The masses of the components are given by $(m_1, m_2, m_3) = (1 M_\odot, 1 M_J, 40 M_J)$ with initial semimajor axes $(a_1, a_2) = (6 \text{ AU}, 100 \text{ AU})$. Recall that Jupiter’s mass $1 M_J = 0.001 M_\odot$. Simulations were run for a variety of initial conditions, specifically the ratio of the semimajor axes α , initial eccentricity e_2 of the outer orbit, and initial mutual inclination i of the two orbits. The eccentricity of the inner orbit e_1 was initially assumed to be nearly circular at 0.001, while e_2 and i were varied.

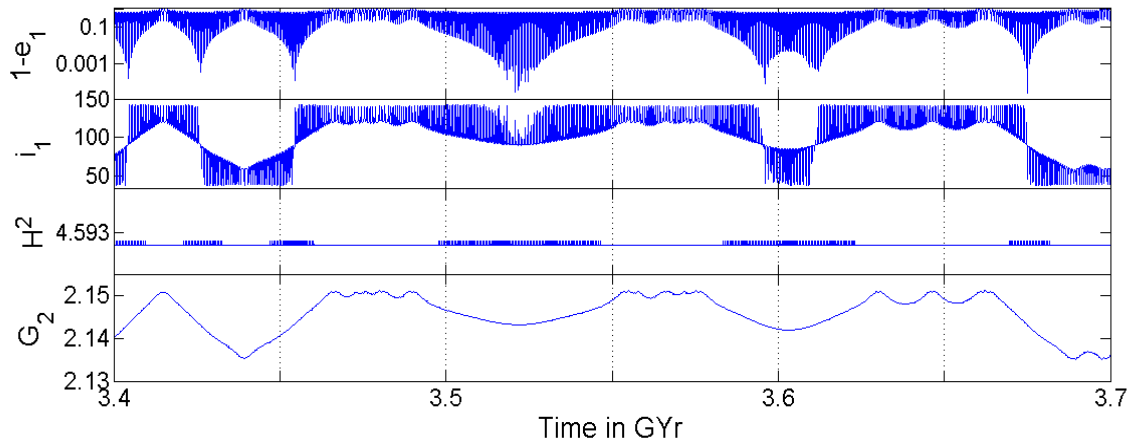
Figure 4 reveals the salient features of octupole-level dynamics. In the first panel we observe periodic spikes in eccentricity of the inner orbit that very strongly correlate with flipping of the inclination i_1 about 90° . Panel b) is a magnification of the first. Notice that the dominant behavior that causes a flip in inclination is indeed the eccentricity of the inner orbit, even though there exist a few surprising cases (for example in the last panel) where a spike does not cause a flip. It should be noted that despite small changes in initial conditions, the prograde versus retrograde behavior of the inner orbit tends to an equilibrium (that is, the system is prograde $\sim 50\%$ of the time). In addition to the occurrence of previously defined Kozai cycles, we now observe a longer envelope which we define as the *octupole-level envelope*, whose time t_8 we shall rigorously define in Fig. 6.

We need a more careful study of those maxima in e_1 correlated with flips in eccentricity versus those that are not, and in the process we also seek a relationship between the newly emergent octupole envelopes and the occurrence of flipped orbits. We proceed by considering the maximum values of the eccentricities of the inner orbit that are possible given varying initial conditions in e_2 and i , as shown in Fig. 5. We observe that as e_2 tends to 1 and as i tends to 90° , the maximum e_1 over several Gyr tends to 1. We take this as evidence that globally, given a nearly circular inner orbit, we need the outer perturber to be at least a) highly eccentric or b) extremely inclined (or both a) and b)) in comparison to the inner orbit at some point of its evolution to induce uniquely octupole-level effects in the inner orbit. In fact, this plot reveals even more, because as we have seen in the previous figure and as we shall continue to observe, high e_1 and flipped orbits are highly correlated. Finally, we can isolate two regimes separated by a sharp slope—the regime where flips do not occur at low $e_{2,\text{initial}}$ and i_{initial} and the regime where flips do occur in the ‘valley’ of the landscape.

In Fig. 6 we isolate one of the octupole-level oscillations. Now we can begin to define the octupole and quadrupole timescales, t_8 and t_4 , respectively, and we can begin to compare them. The purple stars indicate the minima of the envelope we recover by considering only the local maxima of e_1 (that is, the maxima associated with the quadrupole-level oscillations discussed in the first paragraph of Sec. 2). This envelope is computationally well-defined for the initial conditions ($e_2 = 0.6, i = 60$) being studied, but this might not be the case as e_1 oscillates ever more chaotically in the ‘valley’ regime seen in the landscape figure. The red



(a)



(b)

Fig. 4: Results from a simulation performed for 4 Gyr initialized with the following conditions: $(m_1, m_2, m_3, a_1, a_2, e_1, e_2) = (1 M_\odot, 1 M_J, 40 M_J, 6 \text{ AU}, 61 \text{ AU}, 0.001, 0.6)$. Panel a) shows the evolution of $\log(1 - e_1)$, i_1 in degrees, the conserved quantity $H^2 = G_{\text{tot}}^2$ (see eq. (5)), and the magnitude of the outer angular momentum G_2 . Panel b) is a magnification of the evolution. Note that during 3.4 – 3.7 Gyr, there is a ‘blunt’ spike in eccentricity with no flip in inclination.

star indicates the maximum of the envelope defined from one purple star to the next. A cursory glance at the previous Fig. 4 reveals that among all the maxima of the quadrupole-level oscillations, these in particular are correlated with a flipped orbit. As shown in panel b) of that plot, we also observe that not every envelope contains a spike resulting in a flipped e_1 . We pursue this idea in the next figure.

In Fig. 7 we begin comparing the quadrupole timescales t_4 among envelopes versus $1 - e_{1,\text{max}}$, where we define $e_{1,\text{max}}$ by the value of the eccentricity given by the red star as shown in the previous plot. In panel a), for each value of $1 - e_{1,\text{max}}$ we plot three different timescales: the maximum t_4 to be found in the envelope, the minimum t_4 , and the average t_4 . Immediately

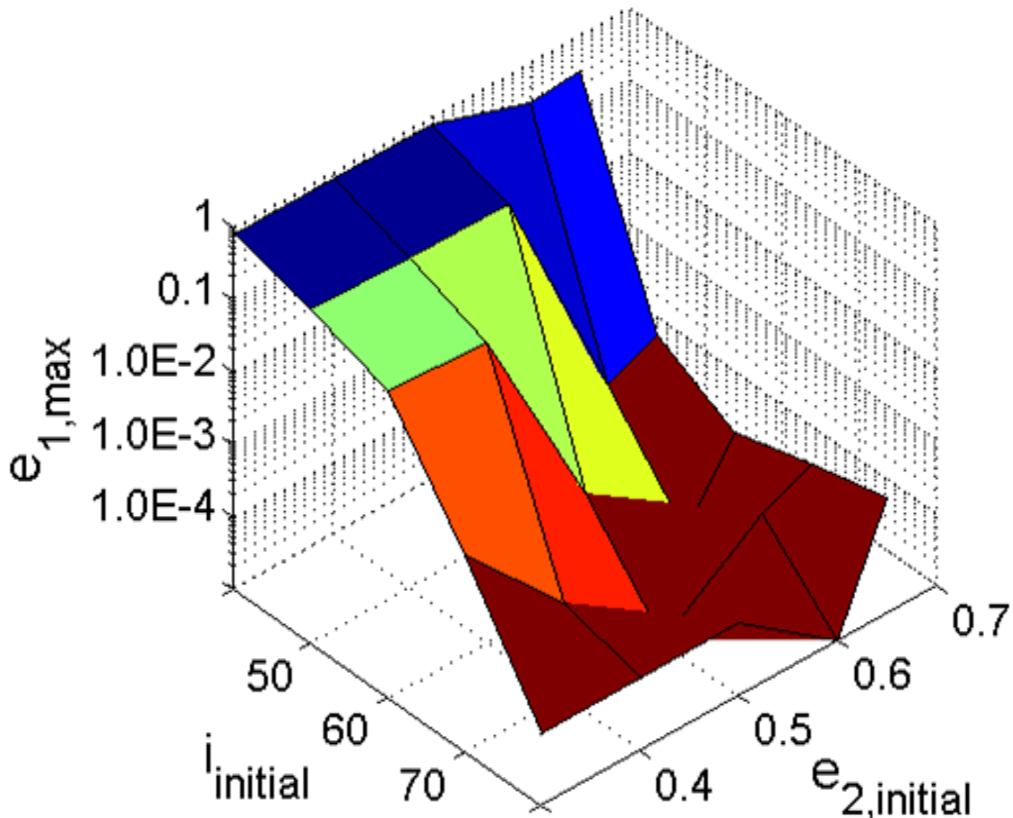


Fig. 5: We plot the surface $1 - e_{1,\max}$ as a function (in z) of the initial e_2 and i after timescales of at least 2 Gyr. We plot points at the grid intersections and interpolate in the obvious (planar) way. As $e_{2,\text{initial}} \rightarrow 1$ and $i_{\text{initial}} \rightarrow 90^\circ$, the likelihood that the system exhibits flipping behaviors tends to 1. Other initial conditions are identical to those in figure 4. As we have determined $e_{1,\max}$ to be equal to 1 (up to numerical error) in some simulations, we set $1 - e_{1,\max}$ to be equal to 10^{-6} for those instances, accounting for the jaggedness as $e_{1,\max}$ becomes very small.

apparent is the gap of two orders of magnitude in e_1 separating envelopes which cause a flip in e_1 versus those that do not. Clearly the most important aspect of the spike in eccentricity of the inner orbit is how high the eccentricity becomes. This was suspected to be the case, but there is more information to be gleaned from panel a). While the maximum values of Kozai timescales appear evenly spread irrespective of flipping behavior, the average and minimum t_4 appear to lie on a curve of increasing derivative with respect to $1 - e_{1,\max}$. This surmise is borne out in panel b) when we instead plot the value of *every* t_4 versus its $1 - e_1$ value in the data set. The fact that the minimum values of t_4 in panel a) appear to lie on the same curve leads us to the conclusion that the exact quadrupole spike correlated with the flip in i_1 is not only the highest, but also one of the fastest (i.e., has the smallest t_4) in the envelope. That the average values also appear to lie on a curve of increasing derivative implies that most of the Kozai cycles in an octupole envelope are ‘bunched’ near the maximum, and only begin to lengthen at the troughs of the octupole-level oscillation (which can be gleaned by a cursory inspection of the isolated octupole envelope in the previous figure). Finally in panel

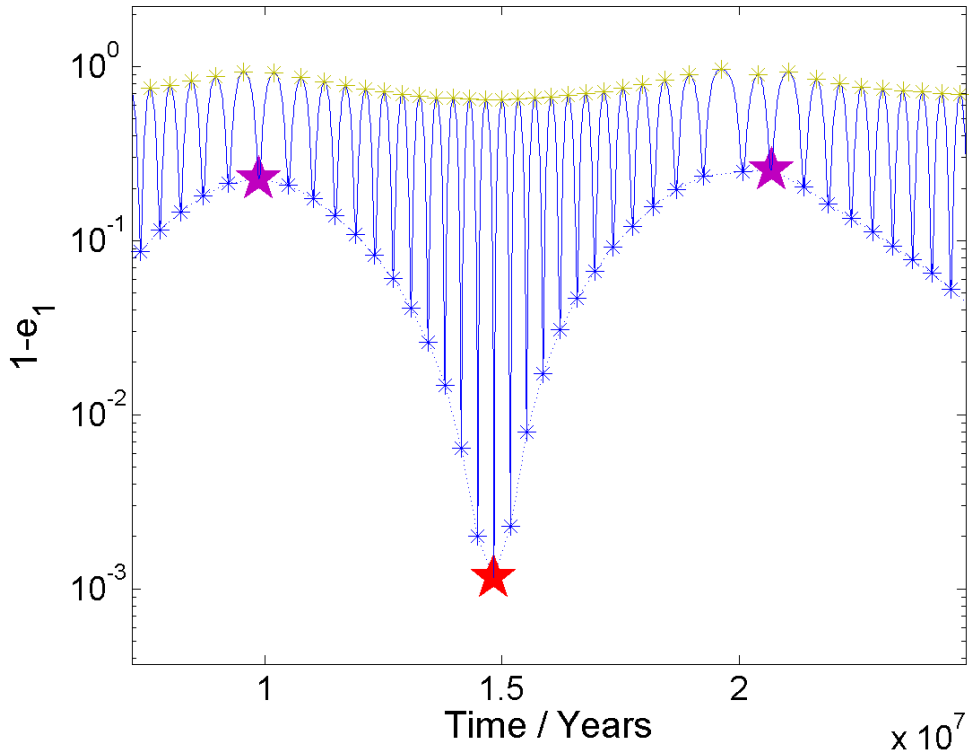


Fig. 6: We identify the datasets we will be using for the figures that follow. In this figure we isolate an octupole-level e_1 oscillation. We define the *octupole time* t_8 of the envelope as the difference in time between the two datapoints denoted by purple stars. The red star is the location of the local maximum of the envelope. Smaller blue asterisks denote the local maxima of the *quadrupole-level* Kozai oscillations. Notice that each Kozai oscillation is bounded on both ends by olive asterisks in the figure. We define the *quadrupole time* t_4 , the time of the oscillation, by the difference in time between neighboring olive asterisks.

c) we magnify the region in which flips occur. Rather than a sharp cut-off between flipping and non-flipping behaviors, we observe instead an increase in statistical likelihood, as we move to the left of the plot, that a flip will occur. This apparent non-determinism is not unexpected in a complex system of many variables: it is likely that sensitive dependence on initial conditions leads the dynamics to chaotically wander near to the appropriate region in the many-dimensional phase space, the result of which is that transitions in i_1 occur with a well-defined statistical distribution.

We wish to continue exploring the apparent long-tail distribution suggested by panel c) of the previous figure, but before we do so we explore other comparisons between the obvious arbiter distinguishing flipping versus non-flipping behavior (i.e., the gap in e_1) and other relevant variables. Our aim is to secure secondary relationships that can accurately help us determine whether an orbit flips or not. In Fig. 8a we plot the timescale of the octupole envelope t_8 versus $1 - e_{1,\max}$ of the envelope. Apart from the horizontal multiscale gap in e_1 , we observe a global contradiction to our local example in Fig. 4 of a relatively wide envelope that does not induce a flip: the envelopes that induce flips in e_1 are on average *longer*

than those that do not induce flips. Coupled with the data from Fig. 7c, we surmise that there must be sufficiently many Kozai cycles in an envelope acting to steadily and quickly reduce i_1 , so that the inner orbit flips before e_1 has time to decay to the trough of its cycle. However, the analytic reasoning to support this claim is obscure because of the complexity of the equations of motion.

In panels b) and c) we make two more attempts to isolate secondary constraining behaviors. In panel b) we plot H_1/H_2 versus $1 - e_1$ for every data point in the set across several Gyr. The envelope of the cone-shaped object in the panel depends heavily on the fact that $H_1 = G_1 \cos i_1 = L_1 \sqrt{(1 - e_1^2)} \cos i_1 = H_1(e_1)$. We are in fact plotting a function of e_1 versus e_1 , so we retrieve very little new information in this plot. We do obtain a weak bound on flipping behaviors of $|H_1/H_2| \lesssim 10^{-3}$ inside the total allowed space of $|H_1/H_2| \lesssim 5 \times 10^{-3}$, which may be broken as $t \rightarrow \infty$. Finally, in panel c) we plot C_3/C_2 versus $1 - e_{1,\max}$ for flipping versus non-flipping envelopes. C_2 and C_3 are the coefficients of the quadrupole and octupole terms, respectively, of the Hamiltonian [eq. (9)] and the resulting equations of motion, so can be considered to be an indicator of their influence on the resulting orbital dynamics. Recent work suggests that for a flip to occur, C_3 and C_2 terms must become comparable for the octupole to become strong enough to force a flip. In panel c) we find that C_3 and C_2 are comparable within an order of magnitude, but no more so than usual if we compare them across all possible datapoints, and not in any obvious way that distinguishes flipping from non-flipping behavior (although we can argue that statistically, flipping behaviors occur at some ill-defined ‘average’ region of $C_3/C_2 \approx -0.348$ that non-flipping points do not enter).

We return to the conjecture presented in Fig. 7 that the number of t_4 cycles is correlated with flipping behavior. In Fig. 9 we plot another octupole-level comparison of the *number* of t_4 cycles within a t_8 envelope versus $1 - e_{1,\max}$. Surprisingly, we can begin to glean a secondary relationship among t_4 , t_8 , and $e_{1,\max}$. Statistically we bear out the conjecture that the number of t_4 oscillations cannot be too low, or a flip will not occur, and if the number of oscillations is too high then a flip will occur. However, within the region of ~ 30 quadrupole oscillations it is not certain (apart from considering $e_{1,\max}$) whether a flip will occur or not. From this we infer that there is still another relationship among the other variables of the system that determines the two behaviors more sharply.

Finally we analyze the long-term behavior of $e_{1,\max}$. We plot in Fig. 10 cumulative distributions of e_1 after runs of at least 2 Gyr comparing two datasets of initial conditions $e_2 = 0.6$ and $e_2 = 0.5$ with all other initial conditions left identical. In panels a–c) we observe that while the total dataset exhibits a slight shift upward for $e_1 \gtrsim 0.21$ and downward for $e_1 \lesssim 0.21$ (obtaining a higher expectation of a higher eccentricity of the inner orbit) as we increase the initial eccentricity of the outer orbit, the difference in eccentricities inducing flips is far more dramatic. For example, reading panel c) we observe that about 50% of flips are caused by $e_1 \leq 0.9996$, if we begin with a higher initial eccentricity of the outer orbit $e_2 = 0.6$, while less than 25% of flips are caused by values of e_1 within those bounds if we begin with a lower initial eccentricity $e_2 = 0.5$. Furthermore, this is true over virtually the entire range of eccentricities of the two datasets where flips occur. This difference is startling, and since nearby points in the phase space of a Hamiltonian system are expected to lie on trajec-

tories exhibiting qualitatively similar dynamics, the difference further supports the claim that there should be a more complex relationship among the orbital elements that provides constraints on the kinds of envelopes that induce flips and therefore retrograde orbits. The last observation we make for this figure is the presence of long tails in the distributions of both datasets in panel a). This indicates that if we wait long enough (i.e., as $t \rightarrow \infty$), an eccentricity of the inner orbit arbitrarily close to 1 can be attained.

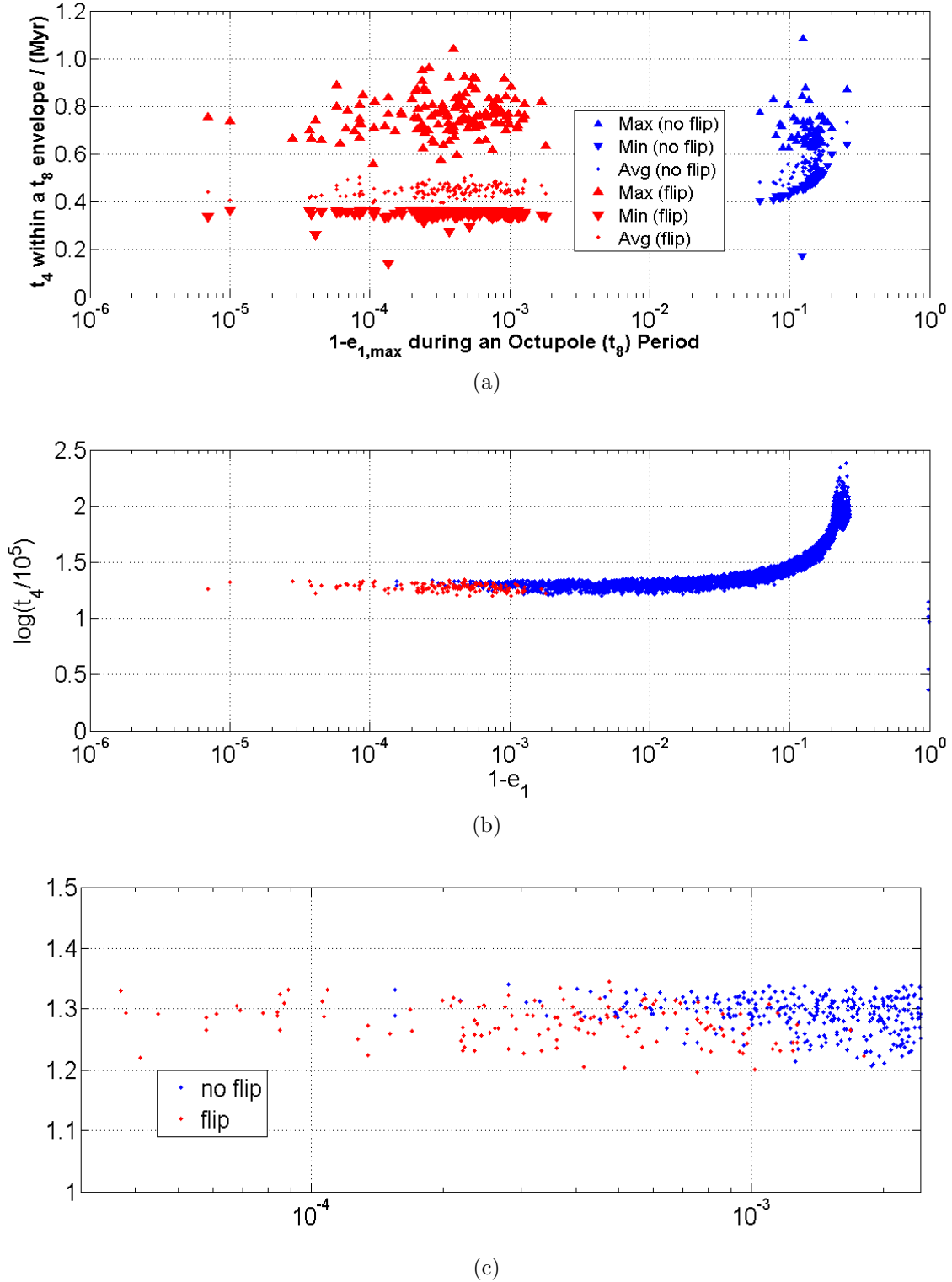


Fig. 7: In panel a) we plot for every octupole-level time interval t_8 (as defined in Fig. 6) a set of three data points: the maximum, minimum, and average length in years of a t_4 cycle versus $1 - e_{1,\max}$, where $e_{1,\max}$ is the value of the eccentricity given by the red star in the prior plot. Notice that the points for which flips occur are clearly separated by a difference of e_1 of two orders of magnitude. The gap in the first panel is not well understood, and is a feature unique to octupole-level effects. This is demonstrated in panel b), where we close the gap by plotting the *entire* dataset (without grouping in t_8 -envelopes) over several Gyr. The upward sloping behavior seen in a) is readily apparent in b), leading us to conclude that the Kozai cycle correlated with the maximum value of t_8 is in fact the shortest. In panel c) we magnify the plot in panel b) to focus on the tail. Note that the cutoff is not sharp. This may be evidence that the system chaotically wanders through its parameter space.

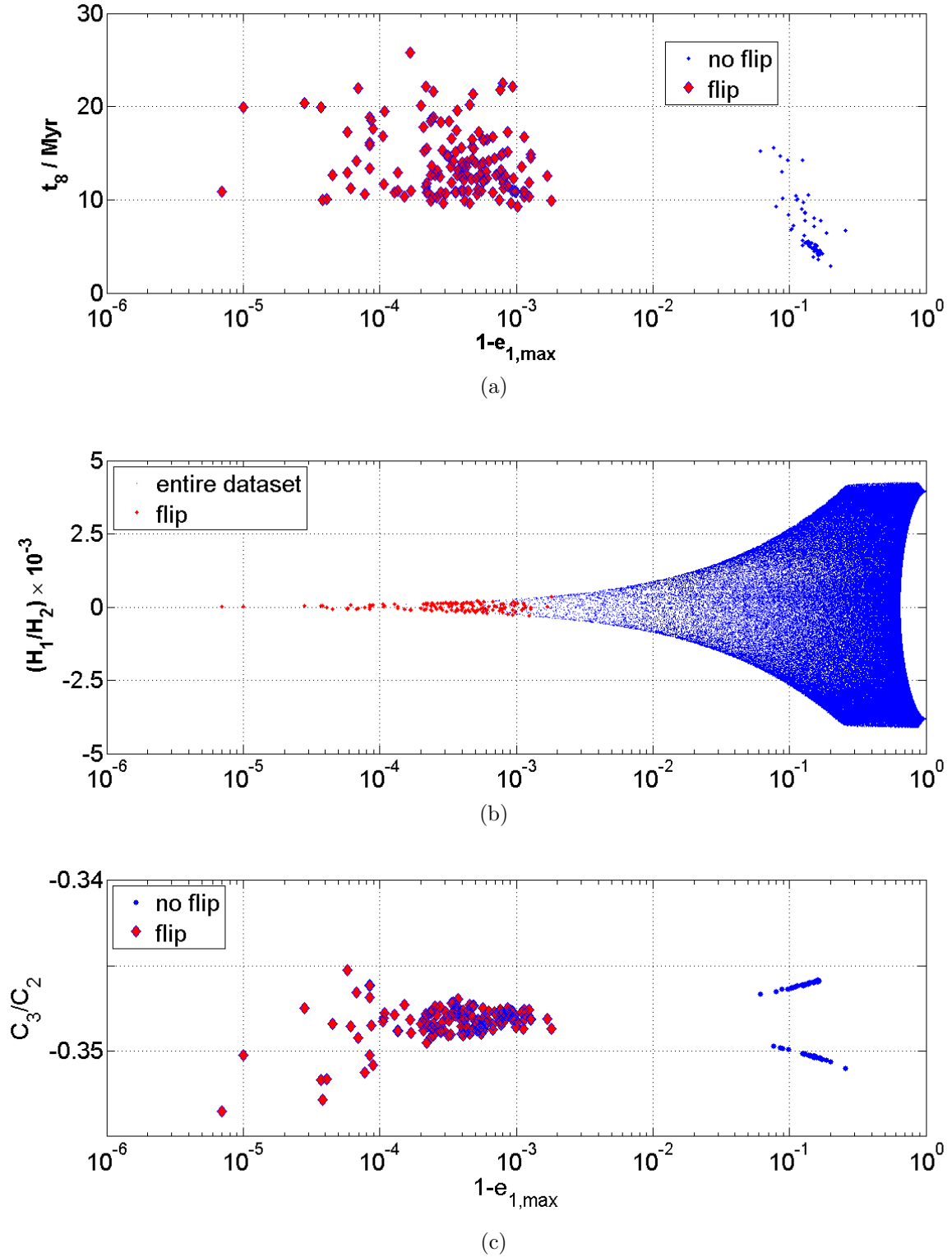


Fig. 8: We continue plotting variables versus $1 - e_{1,\max}$ in an attempt to isolate the relevant quantities determining a flip in i_1 . In panel a) we plot the size of the octupole period t_8 vs $1 - e_{1,\max}$. Note that the behavior observed in Fig. 4b is anomalous: octupole periods are in general longer than usual when a flip occurs. In panel b), we plot H_1/H_2 vs $1 - e_{1,\max}$. Observe that $|H_1/H_2| \lesssim 10^{-3}$ in the flipping regime. This bound may be ‘fuzzy’ in the sense of being broken after an arbitrarily long period of time. Finally we observe in panel c) yet another attempt to tease out the desired relationship, using as the parameter C_3/C_2 . Recall that C_3 leads the octupole terms in the equations of motion [eq. (9)].

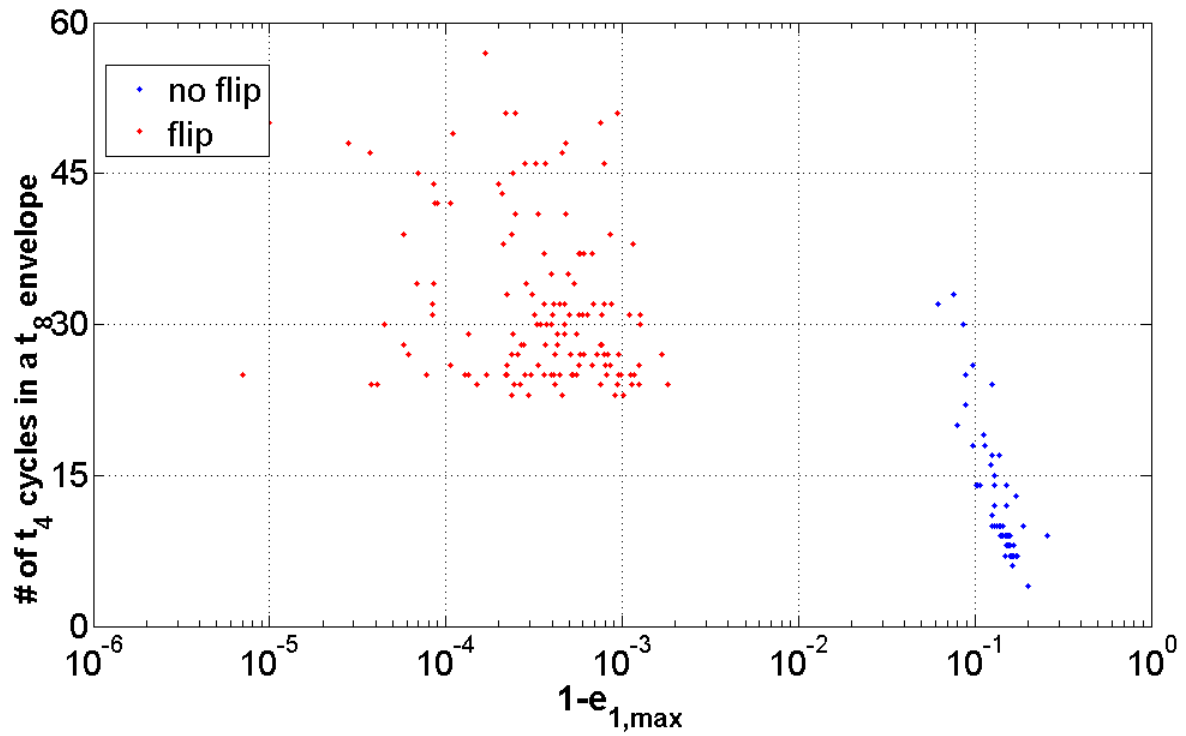
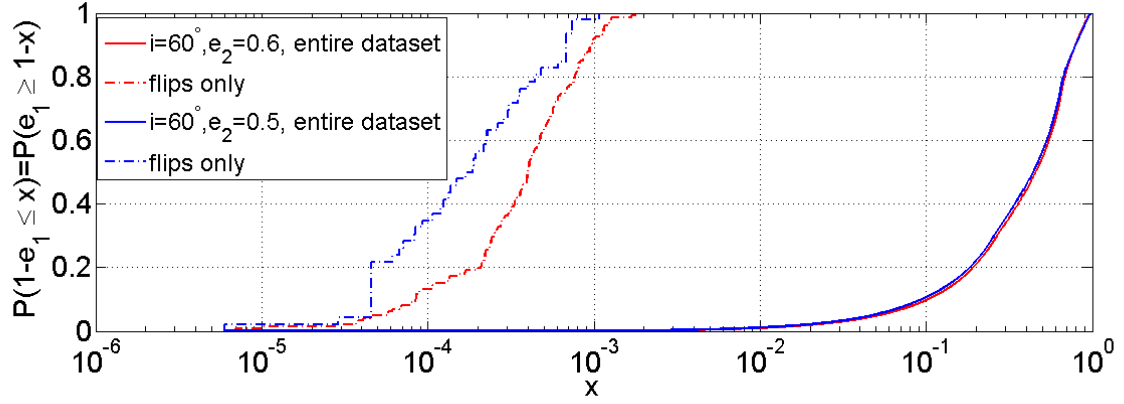
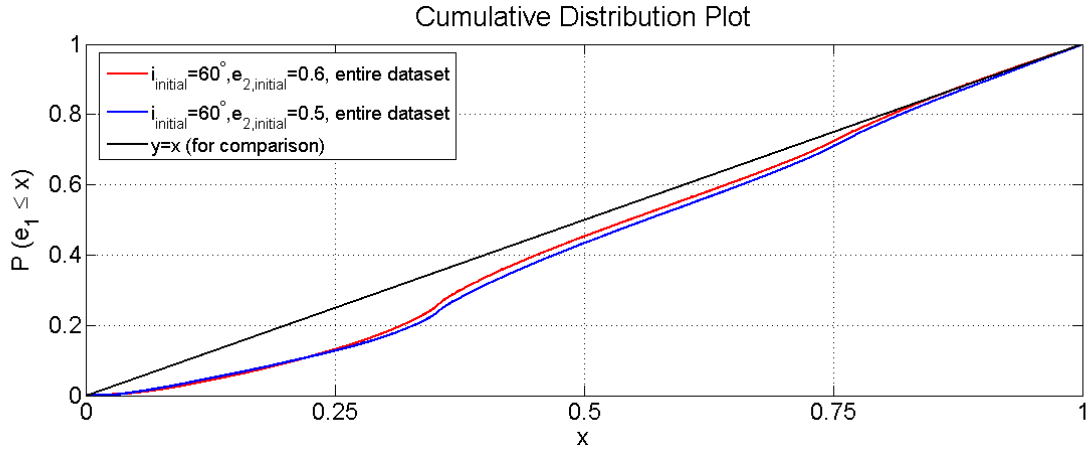


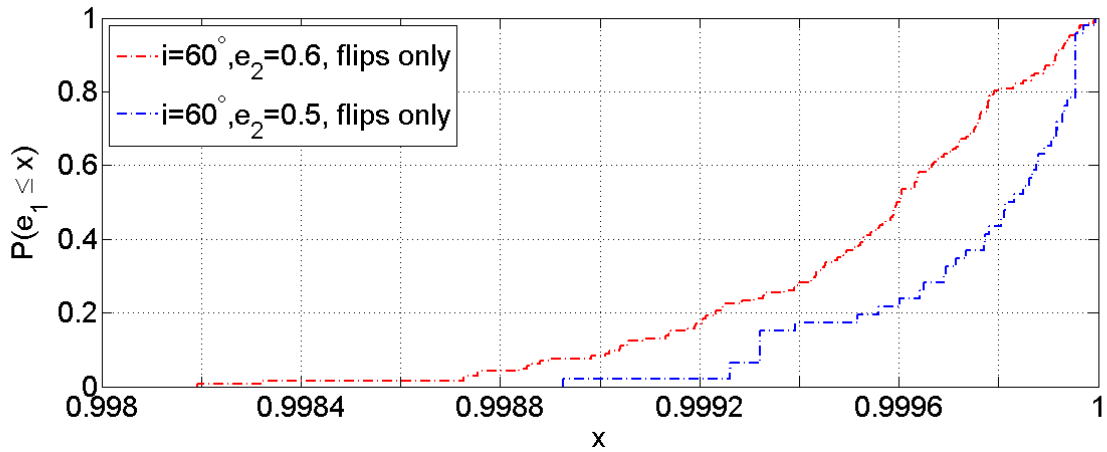
Fig. 9: For each t_8 envelope we plot the number of t_4 oscillations in the envelope versus $1 - e_{1,\max}$ of the envelope. As observed in Fig. 7 as well as Fig. 8a, on average there are *more* oscillations correlated with a flipped inner orbit than usual: we require $\gtrsim 20$ oscillations for a flip to occur. As before, the statistical spread and lack of sharp bounds for the non-flipping orbits indicates a nontrivial dependence on other parameters.



(a)



(b)



(c)

Fig. 10: Cumulative distributions of e_1 for two different initial conditions, $e_2 = 0.6$ (red lines) and $e_2 = 0.5$ (blue lines), are plotted (initial conditions for all other variables remain the same). Notice that for the blue data set, which is deeper inside the region of the landscape where flipping can occur (cf. Fig. 5), it becomes slightly easier to flip the inner orbit in the sense that e_1 need not be quite as high. In panel c), flips can occur for $e_1 \gtrsim 0.9982$ when $e_{2,\text{initial}} = 0.6$, but $e_1 \gtrsim 0.9989$ when $e_{2,\text{initial}} = 0.5$. In panel a), the long tail indicates that if we wait long enough, an eccentricity arbitrarily close to 1 may be obtained; formally, for any $\epsilon > 0$ there exists a time T such that $e_1(t) = 1 - \epsilon$ for some $0 < t < T$.

4 Conclusions

We have presented a detailed numerical analysis of a hierarchical triple containing two planets and a solar-like star, in which we explored the principal relationship between flipping of the inner orbit (producing retrograde motion) and the local maxima of the inner orbital eccentricity e_1 , and we have sought secondary relationships among the other time-dependent variables of the system. The figures presented in Sec. 3 provide important clues to the nature of these relationships. The dependence of flipping on e_1 is obvious, but the nature of the two-order-of-magnitude gap separating flipping from non-flipping behaviors among octupole envelopes remains obscure. It is also clear from the cumulative distributions that even after a large period of time, the dynamics of the hierarchical triple system depend greatly on its initial conditions: a system whose evolution begins further down the ‘valley’ of the landscape of initial conditions where flips occur is more likely to exhibit flips for a given value of e_1 once a certain threshold is crossed.

We can even conjecture two weak probabilistic statements that suggest themselves from the cumulative distributions. First, given two sets of initial conditions that are identical except for e_2 and i (the outer orbital eccentricity and the mutual inclination, respectively), if the values of both e_2 and i for one set of initial conditions are *greater than or equal to* the values for the other set of conditions, then it will be *easier* for the inner orbit to flip in the first case in the sense that the threshold eccentricity will be lower. Secondly, if we are given two sets of initial conditions where the e_1 flipping threshold is lower for the first than for the second, it is also *more probable* for any given e_1 past the threshold to be correlated with a flip in the first set of initial conditions than for the second.

Note that our first conjecture on the conditions for flipping implies the second— a good understanding of the initial conditions immediately gives us qualitative (but unfortunately not quantitative) predictions of the expected behavior of the inner orbit. Notice also that these are ‘lower-bound’ conjectures. The long tails in the eccentricity distributions indicate that ‘upper-bound’ theorems might not exist, and we need to resort to relationships among other variables for further information. We hope to prove these two conjectures analytically, but to do so will require a deeper understanding of the interplay between the variables present in the Hamiltonian equations of motion. We have shown a bound on the ratio of the z-components of the angular momenta H_1/H_2 , but the robustness of this bound given other initial conditions remains a topic for future work. A complete theory will need to explain the surprising lack of information provided by the comparison of the octupole-quadrupole ratio C_3/C_2 vs $1 - e_{1,\max}$. Finally, we hope to extend our results to cases where general relativistic effects and tidal forces play an important role. The qualitative effects of Kozai capture have already been discussed as a possible solution to the retrograde Hot Jupiter problem, but a greater understanding of the analytical nature giving rise to the unique octupole-level dynamics remains elusive.

We can summarize our results in a few points:

- The probability to flip is highly dependent on the maximum inner orbit eccentricity $e_{1,\max}$ just before the flip. The eccentricity threshold that allows a flip depends on the configuration of the system, presumably the semi-major axis ratio $\alpha = a_1/a_2$. We infer this result from a combination of this work and previous calculations. The set of analytical dependences directly derivable from the equations of motion is a topic for future study.
- The probability to reach high eccentricities increases with time (Fig. 10).
- The probability for a flip increases after some eccentricity threshold has been reached (Figs. 7–10).
- The relationship between the quadrupole and octupole time scales (t_4 and t_8 respectively) plays an important role in setting the probability to reach high eccentricities and thus flip the inner orbit (Figs. 7 a and 9). This suggests that in order to reach very high eccentricities the quadrupole time scale (t_4) must be short, and furthermore the number of t_4 oscillations in an octupole envelope must be large.

As a final caveat, we note that we have studied the dynamical behavior of only a few systems, thus exploring a limited area of the relevant parameter space. Future research may confirm whether our results hold over a larger region of the parameter space.

Acknowledgments

I would like to express my heartfelt gratitude to my research advisors, Professor Fred Rasio and Doctor Smadar Naoz, for giving me the opportunity to explore the exciting world of astrophysics through my senior thesis project. For patiently helping me navigate through the world of physics research, I am deeply indebted to you both. Thank you also to Jean Teyssandier for the use of his figure (Fig. 2) and to the other members of the astrophysical theory group for fruitful discussions. Thank you to Professor Lithwick for offering to be my second reader at such short notice. Finally, a warm thank you to my previous advisor, Professor Adilson Motter, for helping me transfer to Professor Rasio’s group and for equipping me with the fundamental research tools that I applied to complete my project.

References

- Blaes, O., Lee, M. H., and Socrates, A. (2002). The Kozai Mechanism and the Evolution of Binary Supermassive Black Holes. *ApJ*, **578**, 775–786.
- Borucki, W. *et al.* (2011). Characteristics of Planetary Candidates Observed by Kepler,II: Analysis of the First Four Months of Data. *ApJ*. arXiv:1102.0541v2.

- Chatterjee, S., Ford, E. B., Matsumura, S., and Rasio, F. A. (2008). Dynamical Outcomes of Planet-Planet Scattering. *ApJ*, **686**, 580–602.
- Eggleton, P. P., Kisseleva-Eggleton, L., and Dearborn, X. (2007). The Incidence of Multiplicity Among Bright Stellar Systems. *Proc. IAU Symp.*, **240**, 347–355.
- Fabrycky, D. and Tremaine, S. (2007). Shrinking Binary and Planetary Orbits by Kozai Cycles with Tidal Friction. *ApJ*, **669**, 1298–1315.
- Ford, E., Kozinsky, B., and Rasio, F. A. (2000). Secular Evolution of Hierarchical Triple Star Systems. *ApJ*, **535**, 385.
- Gaudi, B. S. and Winn, J. N. (2007). Prospects for the Characterization and Confirmation of Transiting Exoplanets via the Rossiter-McLaughlin Effect. *ApJ*, **655**, 550–563.
- Goldstein, H., Poole, C., and Safko, J. (2001). *Classical Mechanics*. Addison Wesley.
- Harrington, R. (1969). The Stellar Three-Body Problem. *Cel. Mech.*, **1**, 200–209.
- Innanen, K. A., Zheng, J. Q., Mikkola, S., and Valtonen, M. J. (1997). The Kozai Mechanism and the Stability of Planetary Orbits in Binary Star Systems. *AJ*, **113**, 1915.
- Kiseleva, L. G., Eggleton, P. P., and Mikkola, S. (1998). Tidal Friction in Triple Stars. *MNRAS*, **300**, 292–302.
- Kozai, Y. (1962). Secular Perturbations of Asteroids with High Inclination and Eccentricity. *AJ*, **67**, 591.
- Lai, D., Foucart, F., and Lin, D. N. C. (2010). Evolution of spin direction of accreting magnetic protostars and spin-orbit misalignment in exoplanetary systems. ArXiv:1008.3148v2.
- Lin, D. N. C. and Papaloizou, J. (1986). On the tidal interaction between protoplanets and the protoplanetary disk. III - Orbital migration of protoplanets. *ApJ*, **309**, 846–857.
- Masset, F. S. and Papaloizou, J. C. B. (2003). Runaway Migration and the Formation of Hot Jupiters. *ApJ*, **588**, 494–508.
- Mazeh, T. and Shaham, J. (1979). The Orbital Evolution of Close Triple Systems – the Binary Eccentricity. *A. & A.*, **77**, 145–151.
- Miller, M. C. and Hamilton, D. P. (2002). Four-Body Effects in Globular Cluster Black Hole Coalescence. *ApJ*, **576**, 894–898.
- Nagasawa, M., Ida, S., and Bessho, T. (2008). Formation of Hot Planets by a Combination of Planet Scattering, Tidal Circularization, and the Kozai Mechanism. *ApJ*, **678**, 498–508.
- Naoz, S., Farr, W., Lithwick, Y., Rasio, F., and Teyssandier, J. (2011). Retrograde hot jupiters from secular planet-planet interactions. *Nature*. arXiv:1011.2501v2.
- Perets, H. B. and Fabrycky, D. C. (2009). On the Triple Origin of Blue Stragglers. *ApJ*, **697**, 1048–1056.

- Perets, H. B. and Naoz, S. (2009). Kozai Cycles, Tidal Friction, and the Dynamical Evolution of Binary Minor Planets. *699*, L17–L21.
- Pribulla, T. and Rucinski, S. M. (2006). Contact Binaries with Additional Components. I. The Extant Data. *AJ*, **131**, 2986–3007.
- Takeda, G., Kita, R., and Rasio, F. A. (2008). Planetary Systems in Binaries. I. Dynamical Classification. *ApJ*, **683**, 1063–1075.
- Tokovinin, A. A. (1997). On the Multiplicity of Spectroscopic Binary Stars. *Astronomy Letters*, **23**, 727–730.
- TriAUD, A. H. M. J., Collier Cameron, A., Queloz, D., Anderson, D. R., Gillon, M., Hebb, L., Hellier, C., Loeillet, B., Maxted, P. F. L., Mayor, M., Pepe, F., Pollacco, D., Ségransan, D., Smalley, B., Udry, S., West, R. G., and Wheatley, P. J. (2010). Spin-orbit angle measurements for six southern transiting planets. New insights into the dynamical origins of hot Jupiters. *A. & A.*, **524**, A25.
- Valtonen, M. and Karttunen, H. (2006). *The Three-Body Problem*. The Cambridge University Press.
- Verrier, P. and Evans, N. (2008). High inclination planets and asteroids in multistellar systems. *Mon. Not. R. Astron. Soc.*, **394**, 1721–1726.
- Wang, Q. (1991). The Global Solution of the N-body Problem. *Cel. Mech.*, **50**, 73–88.
- Wen, L. (2003). On the Eccentricity Distribution of Coalescing Black Hole Binaries Driven by the Kozai Mechanism in Globular Clusters. *ApJ*, **598**, 419–430.
- Winn, J. N., Fabrycky, D., Albrecht, S., and Johnson, J. A. (2010). Hot Stars with Hot Jupiters Have High Obliquities. *ApJL*, **718**, L145–L149.
- Wu, Y. and Murray, N. (2003). Planet Migration and Binary Companions: The Case of HD 80606b. *ApJ*, **589**, 605–614.
- Wu, Y., Murray, N. W., and Ramsahai, J. M. (2007). Hot Jupiters in Binary Star Systems. *ApJ*, **670**, 820–825.